Reactions of Laser-Ablated Scandium Atoms with Dioxygen. Infrared Spectra of ScO, OScO, $(O_2)ScO$, $(ScO)_2$, and $Sc(O_2)_2$ in Solid Argon

George V. Chertihin and Lester Andrews*
Department of Chemistry, University of Chemistry, Charlottesville, Virginia 22901

Marzio Rosi[†] and Charles W. Bauschlicher, Jr.
STC-230-3, NASA Ames Research Center, Moffett Field, California 94035

Received: July 29, 1997[⊗]

Laser-ablated Sc atoms react with O_2 during condensation in excess argon to give ScO, OScO, and $(O_2)ScO$ as major products, which are identified from oxygen isotopic substitution on their matrix infrared spectra. The linear suboxide molecule ScOSc is a minor product. Annealing allows further association to form ScO_3, $(ScO)_2$, and $Sc(O_2)_2$. The OScO molecule is bent: based on the oxygen-18 shift in the ν_3 mode, the valence angle is 128 ± 4°. The ν_3 fundamental of OScO at 722 cm^{-1} is substantially lower than the ScO fundamental at 976 cm^{-1}, which is in accord with weaker bonds in the dioxide. Similar reactions in excess nitrogen give evidence of extensive ligation.

Introduction

Reactions of laser-ablated first row transition metal atoms and oxygen molecules have been extensively studied in this laboratory.[1−10] The main products of oxidation are the monoxide and dioxide molecules. Transition-metal dioxygen molecules can exist in three isomeric forms—the bent or linear insertion product, and side-bonded and end-bonded dioxygen complexes.[2,3] The coexistence of two or three isomers is characteristic of the middle and late transition metals Cr, Mn, Fe, Co, Ni and Cu, while the early transition metals Ti and V form only bent dioxides.[1−10] Among the oxides of scandium only ScO has been thoroughly investigated in the gas phase and matrixes probably due to its appearance in the spectra of stars.[11−21] Scandium with three valence electrons and low atomic number is also very convenient for ab initio calculations, and a number of theoretical studies have been devoted to this molecule.[22−25]

Almost all gas phase work found that Sc reacting with O_2 forms ScO and does not insert into oxygen although a rather large exothermicity for OScO formation has been predicted by comparison with rare earth oxide thermochemistry.[26] However, in contrast matrix isolation studies reported OScO as a bent molecule with accidental degeneracy of symmetric and antisymmetric vibrations.[20] The dioxide is difficult to make in the gas phase, and a recent thermochemical study employed the ScO^+ reaction with NO_2.[27] The matrix work assigned frequencies in the same range for ScO (970 cm^{-1}) and OScO (905 cm^{-1}), but mass spectrometry found the Sc−O bond in the dioxide to be much weaker than in the monoxide.[20,27] Thus, it was decided to reinvestigate the Sc + O_2 system using laser ablation as a source of Sc atoms in order to prepare the dioxide molecule. A particularly relevant laser vaporization investigation of Sc_2O_3 produced a fast beam of scandium atoms and monoxide.[28]

The present work shows that scandium is an unusually interesting transition metal. Its chemistry is related to the chemistries of Ca and Ti as might be expected. For example, scandium forms a symmetrical bent OScO dioxide molecule in both argon and nitrogen matrixes with valence angle and strong ν_3 fundamental intermediate between OCaO and OTiO values.[1,29,30] The large difference between ScO and OScO frequencies found here is also comparable to CaO and OCaO in contrast to TiO and OTiO. One of the remarkable properties of ScO is its ability to form complexes with dioxygen and dinitrogen. Moreover, ground state Sc does not react with oxygen to form the bent dioxide molecule, like Ca in contrast to Ti, but metastable Sc atoms produced here by laser ablation insert into oxygen. Generally speaking, scandium, the first transition metal, inherits a lot from calcium which contributes to its unusual chemistry.

Experimental Section

The technique for laser ablation and FTIR matrix investigation has been described in detail.[1−4] Scandium (Johnson Matthey, lump, 99.9%) was mounted on a rotating (1 rpm) stainless steel rod. The Nd:YAG laser fundamental (1064 nm, 10 Hz repetition rate, 10 ns pulse width, 20−50 mJ pulses) was focused on the target through a hole in the CsI cryogenic (10 K) window. Metal atoms were co-deposited with 0.2−1% O_2/Ar, O_2/N_2 (and their isotopic modifications) and N_2O/Ar at 2−4 mmol/h for 1−3 h periods. FTIR spectra were recorded with 0.5 cm^{-1} resolution on a Nicolet 750 instrument. Matrix samples were temperature cycled, and more spectra were collected; selected samples were subjected to broadband photolysis by a medium-pressure mercury arc (Philips, 175 W) with globe removed (240−580 nm).

Theoretical Section

DFT-based calculations were done for small scandium oxide molecules using the Gaussian 94 program system.[31] The 6-31+G* basis sets are used for oxygen and nitrogen.[32] For Sc [8s 4p 3d] contraction of the (14s 9p 5d) primitive set developed by Wachters was employed.[33] The s and p spaces are contracted using contraction number 3, while the d space is contracted (311). To this basis set one diffuse p function with exponent 0.13462 is added; this is the tight function optimized by Wachters multiplied by 1.5. The second, more diffuse, p

---

[†] Permanent address: Department of Chemistry, University of Perugia, I-06100, Perugia, Italy.

[⊗] Abstract published in *Advance ACS Abstracts,* November 15, 1997.

S1089-5639(97)02482-1 CCC: $14.00

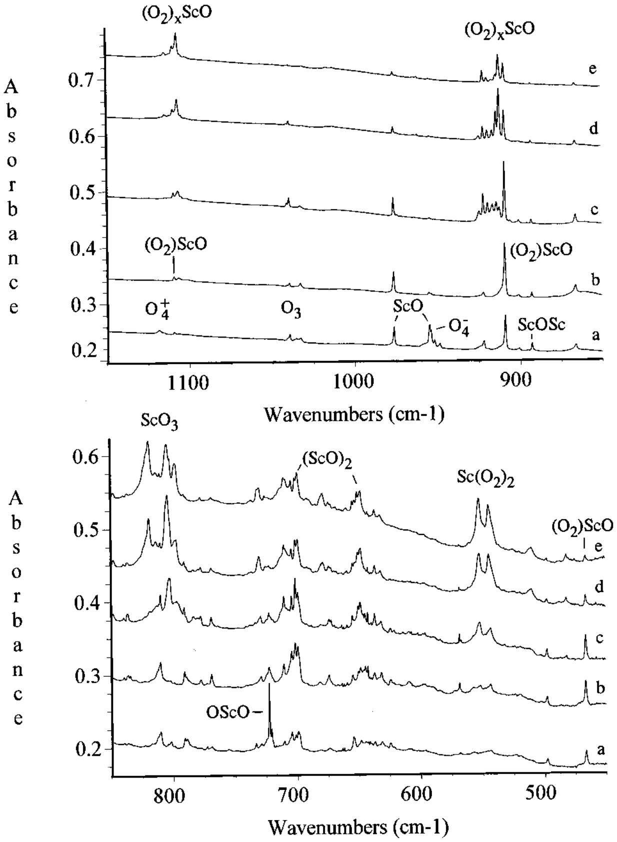

Figure 1. Infrared spectra in the 1150−450 cm^{-1} region for laser-ablated Sc atoms co-deposited with 1% O_2 in argon at 10 K. (a) sample deposit for 1 h, (b) after 240−580 nm photolysis for 25 min, (c) after annealing to 25 K, (d) after annealing to 35 K, and (e) after annealing to 40 K.

TABLE 1: Absorptions (cm^{-1}) Observed for Sc + O_2 Reaction Products in Condensing Argon

$^{16}O_2$	$^{18}O_2$	$^{16}O_2 + {}^{16}O^{18}O + {}^{18}O_2$	R(16/18)	D/A/Ph^a	assign
1554.3	1467.3	1554.4, 1512.0, 1467.3	1.0594	o + −	$(O_2)ScO_3$?
1039.5	982.3	sextet	1.0582	+ + −	O_3
1109.5	1046.8	1109.5, 1079.4, 1047	1.0599	+ + +	$(O_2)ScO$
1106.8	1045.5	1106.8, 1076.6, 1045	1.0586	o + +	$(O_2)_xScO$
1104.6	1042.5		1.0596	o + +	site
976.3	935.6	976.3, 935.6	1.0435	+ − o	ScO blue site
954.8	915.1	954.8, 915.1	1.0434	+ − −	ScO red site
951.8	912.3	951.8, 912.3	1.0433		site
948.9	909.3	948.9, 909.3	1.0436		site
953.8	901.7	940.5, 928.3, 925.1, 914.4, 901.7	1.0578	+ − −	O_4^-
922.0	883.5	922.0, 883.5	1.0436	+ −	$(O_2)ScO$
921.8	883.2	921.4, 883.6	1.0437	o + −	$(O_2)_xScO$
919.2	880.8	918.9, 881.0	1.0436	o +	site
916.3	878.0	916.3, 878.2	1.0436	o +	site
913.9	875.8	913.5, 876.0	1.0435	o +	site
912.0	873.9	911.6, 874.3	1.0436	o +	$(O_2)_xScO$
909.0	871.2	908.8, 871.3	1.0434	+ + +/−	$(O_2)ScO$
892.9	850.4	892.9, 850.4	1.0500	+ − −	ScOSc
866.0	828.7	865.5, 830.3	1.0450	+ − +	ScOScO
847.8	812.7	847.8, 812.7	1.0432	o + −	?X−ScO
818.6	773.8	803.7, 795.4, 785.7	1.0579	o +	site
804.0	759.2	779.2, 769.4, 759.3	1.0590		ScO_3
797.6	753.3		1.0588		site
809.9	776.0		1.0437	+ − +	$ScO(O_2)$?
768.9	737.4		1.0427	+ − +	?X−ScO
733.3	706.8		1.0375	+ − −	OScO site
722.5	696.9	722.5, 704.9, 696.9	1.0367	+ − −	OScO (ν_3)
704.2	675.7		1.0422	+ − o	$(ScO)_2$ site
699.1	670.1	699.1, 684.8, 670.1	1.0430	o +	$(ScO)_2$
653.8	626.6		1.0434	+ − o	?
647.8	622.5	647.8, 631.5, 622.5	1.0425	o +	$(ScO)_2$
552.6	536.2	547.7, 538.0, 529.5	1.0306	o +	$Sc(O_2)_2$
544.6	528.6		1.0304	o +	site
497.8	474.9	497.8, 486.7, 474.9	1.0482	+ + +	?
481.9	461.5		1.0442	+ + +	?
466.3	451.2	466.1, 461.3, 451.7	1.0332	+ + +	$(O_2)ScO$

[a] D, A, Ph denote presence on sample deposition, annealing behavior, and photolysis behavior.

function is not included as it was found to affect results very slightly, but introduced severe convergence problems to the orbital optimization procedure. The Hay diffuse d function with exponent 0.0588 is also added.[34]

In general the B3LYP and BP86 functionals[35−37] yield similar frequencies. ScO_2 is an exception to this trend, where BP86 yields significantly better frequencies. For example, at the BP86 and CCSD(T) levels of theory, the $^2B_2$ state of ScO_2 has two equivalent bonds with bond order of 1.5. The B3LYP functional incorrectly yields inequivalent bonds, one with a bond order of 1 and the other with a bond order of 2. Since a similar situation can exist for other states of ScO_2, we use the BP86 functional for all of these systems.

Results

FTIR spectra of the Sc + O_2/Ar, Sc + O_2/N_2, and Sc + N_2O/Ar systems and density functional calculations will be presented.

Sc + O_2/Ar. Spectra are shown in Figure 1 and listed in Table 1. The most intense bands after deposition were 976.3, 954.8, 909.0, 892.9, 866.0 and 722.5 cm^{-1}. The 976.3 and 954.8 cm^{-1} bands decreased on annealing and the latter band also disappeared on full arc photolysis. The 909.0 cm^{-1} band increased on photolysis and subsequent annealing up to 25 K and decreased on further annealing. New bands in the 925−900 cm^{-1} region appeared in the spectra after annealing together with bands around 1110 cm^{-1} (a weak 1109.5 cm^{-1} band was observed after deposition and behaved similarly to the 909.0 cm^{-1} band). The 892.9 and 722.5 cm^{-1} bands decreased on annealing and broadband photolysis, while the 866.2 cm^{-1} band increased on photolysis and annealing up to 25 K and decreased with increasing temperature. The strong new bands near 820−800, 700, 650 and 550 cm^{-1} appeared in the spectra only after annealing.

Oxygen isotopic substitution was employed for band identification. All bands in the 1000−850 cm^{-1} region produced doublets with both mechanical ($^{16}O_2 + {}^{18}O_2$) and statistical ($^{16}O_2 + {}^{16}O^{18}O + {}^{18}O_2$) mixtures (Figure 2). The 1109.5, 722.5, 699.1, 647.8 and 466.3 cm^{-1} bands produced doublets and triplets, the 820−800 and 550 cm^{-1} bands produced quartet and triplet structures, respectively, with the mechanical mixture. With scrambled oxygen strong overlapping was observed in the latter isotopic structures, and unresolved sextets are assumed.

Sc + N_2O/Ar. Supplemental experiments were done with the N_2O/Ar mixtures. After deposition similar strong 976.3, 954.8, 866.0, and 722.5 cm^{-1} bands were observed, and the yield of the first three bands was enhanced compared with the O_2 system. Instead of the strong 909.0 cm^{-1} band and its blue-shifted satellites, an 894.9 cm^{-1} band and satellites in the 909−900 cm^{-1} region appeared in the spectra. Behavior of all these bands was similar to bands in the O_2 experiments; however, no bands were observed around 1110 cm^{-1}. The 722.5, 704.2 and 647.8 cm^{-1} bands also appeared in the spectra after deposition; the first band increased and other bands decreased on annealing, while new broad features around 690 and 640 cm^{-1} grew with increasing temperature.

Sc + O_2/N_2. Spectra of the nitrogen matrix system are shown in Figure 3 and listed in Table 2. Weak NO and NO_2 bands were observed.[38] Deposition revealed a strong doublet at 710.2/705.4 cm^{-1}, which decreased on annealing while other bands

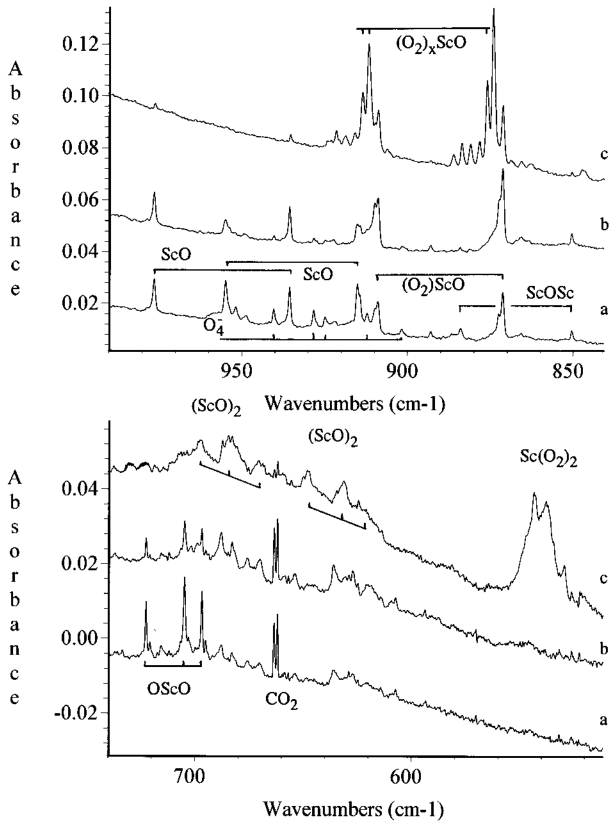

Figure 2. Infrared spectra in the 990−840 and 740−510 cm^{-1} regions for laser-ablated Sc atoms co-deposited with statistical isotopic oxygen 0.25% $^{16}O_2$, 0.50% $^{16}O^{18}O$, 0.25% $^{18}O_2$ in argon at 10 K. (a) sample deposit for 1 h, (b) after 290−580 nm photolysis for 20 min, and (c) after annealing to 35 K.

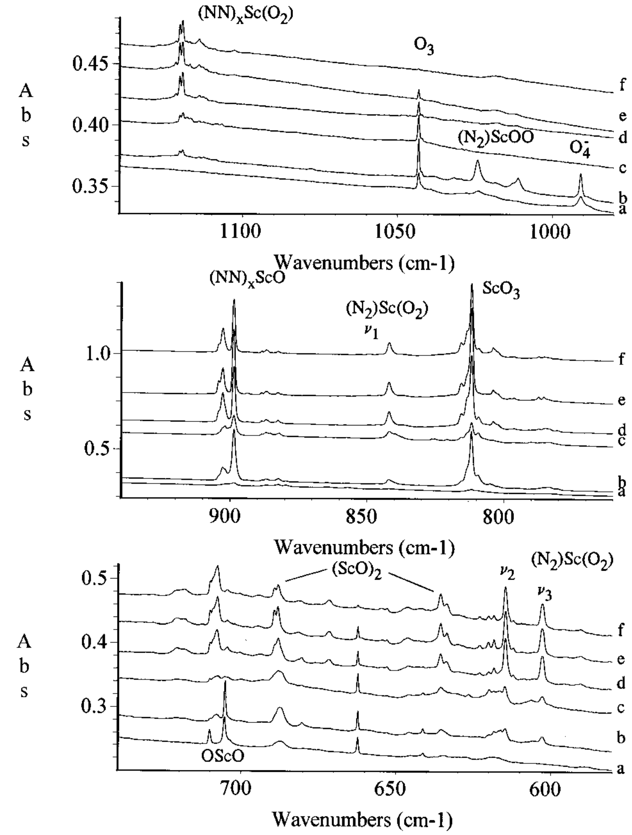

Figure 3. Infrared spectra in the 1140−980, 940−760 and 740−580 cm^{-1} regions for laser-ablated Sc atoms co-deposited with 1% O_2 in nitrogen at 10 K. (a) sample deposit for 1 h, (b) after annealing to 25 K, (c) after 240−580 nm photolysis for 25 min, (d) after annealing to 30 K, (e) after annealing to 35 K, and (f) after annealing to 40 K.

appeared at 1120.4/1119.4, 841.9, 614.6 and 602.8 cm^{-1}. These bands increased on photolysis and annealing in the same proportion. A new 2126.8/2125.3 cm^{-1} doublet in the high frequency region behaved similarly to these bands; annealing changed the intensity distribution of its components in the same way. Weak 1828.2, 1824.6, 1024.1 and 1011.0 cm^{-1} bands observed on deposition grew on annealing to 25 K and disappeared on photolysis. Weak 898.7 and 811.7 cm^{-1} bands always increased markedly on annealing and decreased on photolysis. Weak 707.7, 688.1 and 635.5 cm^{-1} bands in the low-frequency region increased on annealing. Finally, the strong band at 865.0 cm^{-1} observed with scandium in pure nitrogen[39] was not observed here.

Oxygen isotopic substitution revealed the following data. The four bands at 1120.4/1119.4, 841.9, 614.6 and 602.8 cm^{-1}, which appeared only on annealing always produced triplets with both mechanical and statistical mixtures. With the mechanical mixture the intensity distribution was 1:0:1 on deposition and the intermediate component appeared on photolysis after annealing. This triplet decreased on further annealing, decreased on further photolysis and increased on further annealing reaching final relative intensities of approximately 3:2:3 (Figure 4). In the scrambled oxygen experiments the intensity distribution was 1:2:1. The 1024.1/1011.0 cm^{-1} band produced doublet and quartet isotopic structures, respectively, with isotopic mixtures. The 898.7 cm^{-1} band always produced doublets, the 811.7 cm^{-1} band produced quartet and sextet isotopic structures with the ozone-like intensity distribution. The 710.2/705.4, 688.1 and 635.5 cm^{-1} bands produced doublets and triplets, with the mechanical and statistical mixtures, respectively.

Calculations. DFT/BP calculations were done for the small oxides ScO, OScO, $Sc(O_2)$ and ScOO and their dinitrogen complexes, and the results are listed in Table 3. The BP frequency for ScO, 970 cm^{-1}, is in excellent agreement with the 971 cm^{-1} RCCSD(T) value[25] and the 965 cm^{-1} gas-phase value.[11,15] For OScO and $Sc(O_2)$, quartet states were significantly higher in energy than doublet states and examples for OScO and $Sc(O_2)$ are given in Table 3. The doublet end-bonded ScOO species closes to $Sc(O_2)$.

Dinitrogen binds to all of these oxides with energies ranging from 6 to 14 kcal/mol. For ScO, calculations show that end-on ligation by N_2 at 6 kcal/mol red-shifts the fundamental by 51 cm.[1] In the case of cyclic $Sc(O_2)$, the side-on $(N_2)Sc(O_2)$ species is bound to N_2 by 14 kcal/mol whereas the end-on species $NNSc(O_2)$ is bound by 11 kcal/mol, but the oxide submolecule frequencies are little affected in either complex. The open dioxide $NNScO_2$ complex is bound by 8 kcal/mol and the OScO stretching modes are red-shifted by only 14 and 8 cm^{-1}. Although a higher energy species, the $(N_2)ScOO$ complex is a stable minimum.

Discussion

Assignment of spectral bands will be presented.

ScO and Its Complexes with Dioxygen and Dinitrogen. Two bands at 976.3 and 954.8 cm^{-1} always appeared together after deposition and decreased on annealing. The latter band decreased at a faster rate and disappeared on photolysis. Both bands produced doublets with mechanical and statistical mixtures, and the 16/18 ratio 1.0435 is very close to the harmonic ScO diatomic value of 1.0437. These bands have been observed previously: the first band was detected in the spectra of the Sc + O_2/Ar (5%) system,[20] while the second band was found in the spectra of Sc + H_2O in argon[21] and Sc_2O_3 evaporation

TABLE 2: Absorptions (cm^{-1}) Observed for Sc + O_2 Reaction Products in Condensing Nitrogen

$^{16}O_2$	$^{18}O_2$	$^{16}O_2$ + $^{16}O^{18}O$ + $^{18}O_2$	*R*(16/18)	D/A/Ph[a]	assign
2126.8	2126.8			o + +	$(NN)_xSc(O_2)$
2125.3	2125.3			o + +	
1828.2	1828.2			o + −	site
1824.6	1824.6			o + −	$(N_2)ScOO$
1524.3	1488.2	1524.3, 1488.2	1.0243	o + o	Sc^+NO^-
1431.8	1396.3	1431.8, 1396.3	1.0254	o + o	Sc^+NO^-
1193.0	1165.5	1193.0, 1178.4, 1165.5	1.0236	o + −	$Sc^+NO_2^-$
1120.4	1057.2	1120.4, 1089.3, 1057.2	1.0598	o + +	site
1119.4	1056.3	1119.4, 1088.4, 1056.3	1.0597	o + +	$(NN)_xSc(O_2)$
1114.1	1051.3	1114.1, 1083.2, 1051.3	1.0597	o + +	$(NN)_xSc(O_2)$
1024.1	968.7	1024.1, 1004.6, 989.4, 968.7	1.0572	o + −	$(N_2)ScOO$
1011.0	955.9	1011.0, 995 sh, 976.9, 955.9	1.0576	o + −	site
990.7	936.2		1.0582	+ + −	O_4^-
902.7	865.0		1.0436	o + −	$(NN)_xScO$
898.7	861.1		1.0437	+ + −	$(NN)_xScO$
886.8	849.9		1.0437	o + +	$(NN)_xScO$
882.5	845.7		1.0435		$(NN)_xScO$
841.9	798.1	841.9, 819.8, 798.1	1.0549	o + +	$(N_2)Sc(O_2)$ (ν_1)
811.7	766.5	811.7, 802.0, 792.6, 786.7, 776.7, 766.5	1.0590	o + −	ScO_3
803.9	759.9		1.0579	o + −	site
787.3	745.8		1.0556	o + o	?
785.4	743.2		1.0568	o + o	?
710.2	684.8	710.2, 692.8, 684.8	1.0371	+ − −	OScO site
705.4	680.0	705.4, 686.7, 680.0	1.0374	+ − −	OScO (ν_3)
707.7	677.8	707.4, 694.6, 678.0	1.0441	o + o	?
688.1	660.0	688, 673, 660	1.0424	o + +	$(ScO)_2$
641.2	641.2			+ − o	$(ScN)_2$
635.5	610.0	635.5, 619.6, 610.0	1.0418	o + o	$(ScO)_2$
621.7	600.7		1.0350	o + o	$Sc(O_2)$ site
618.3	597.9		1.0341	o + +	$(N_2)_2Sc(O_2)$ site
614.6	593.7	614.6, 605.0, 593.7	1.0352	o + +	$(N_2)Sc(O_2)$ ν_2
609.0	580.3		1.0495	o + o	$(N_2)Sc(O_2)$ site
602.8	573.9	602.8, 586.2, 573.9	1.0504	o + +	$(N_2)Sc(O_2)$ ν_3
461.1	447.9	461.1, 448.0	1.0295	o + +	?

[a] D, A, Ph denote presence on sample deposition, annealing behavior, and photolysis behavior.

products.[19] All earlier work assigned these bands to the ScO molecule, which agrees with the 965 cm^{-1} gas-phase value.[11,15] Note also that one of these bands is blue-shifted 11 cm^{-1} and the other red-shifted 10 cm^{-1} from the gas-phase value and that the CaO fundamental was blue-shifted 24 cm^{-1} in solid argon.[29]

In our experiments these bands were almost of equal intensity with the use of 1% O_2 in argon mixtures, while with 0.5% O_2 intensity ratio was 1:2−1:3. Probably, the high-frequency site could be produced with high oxygen concentration in matrixes. Moreover, the first work used 12−15 K while other works used 10 K and less. It was mentioned above that the second band decreased at a faster rate on annealing than the first one. Thus, the first work[20] did not observe the 954.8 cm^{-1} band simply due to higher temperature of deposition. It is necessary to emphasize that these bands are blue and red matrix sites of ScO in solid argon, not complexes of ScO and oxygen. They were also observed in the spectra of Sc + N_2O/Ar system and enhanced compared with the oxygen system, which is expected taking into account the exothermicity of reactions 1 and 2.

$$Sc + O_2 \rightarrow ScO + O \qquad \Delta H = -43 \text{ kcal/mol} \qquad (1)$$

$$Sc + N_2O \rightarrow ScO + N_2 \qquad \Delta H = -120 \text{ kcal/mol} \qquad (2)$$

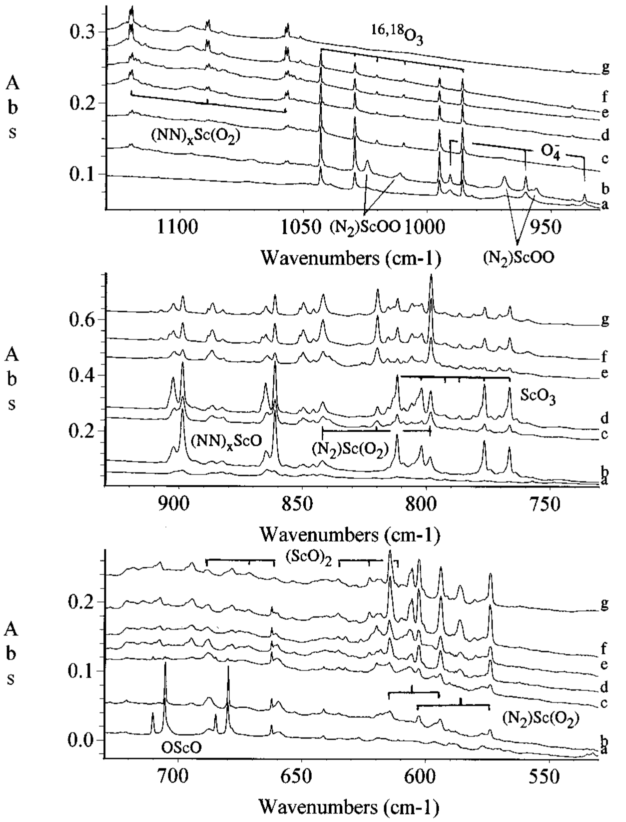

Figure 4. Infrared spectra in the 1130−930, 930−730 and 730−530 cm^{-1} regions for laser-ablated Sc atoms co-deposited with mixed isotopic oxygen 0.6% $^{16}O_2$ + 0.6% $^{18}O_2$ in nitrogen at 10 K. (a) sample deposit for 1 h, (b) after annealing to 25 K, (c) after 240−580 nm photolysis for 25 min, (d) after annealing to 30 K, (e) after 240−580 nm photolysis, (f) after annealing to 35 K, and (g) after annealing to 40 K.

TABLE 3: Frequencies, Infrared Intensities, and Structures Calculated for Small Scandium Oxides and Their Dinitrogen Complexes Using Density Functional Theory (BP)

ScO	$^2\Sigma^+$	1.676 Å	970 (155)[a]
NNScO	D	1.692 Å	1932 (4990), 919 (250), 271 (128)
OScO $E = 0^b$	$^2B_2$	1.782 Å 125.9°	742 (a_1, 44), 545 (b_1, 7), 115 (a_1, 55)
$Sc(O_2)$ $E = +33^b$	$^2A_1$	1.870 Å 1.494 Å	882 (a_1, 90), 634 (a_1, 24), 570 (a_1, 9)
$Sc(O_2)$ $E = + 42$	$^4A_2$	2.108 Å 1.348 Å	1141 (a_1, 24), 472 (a_1, 48), 349 (b_1, 3)
OScO $E = +75$	$^4B_2$	1.909 Å 129.9°	537 (a_1, 58), 488 (b_1, 17), 131 (a_1, 28)
$NNScO_2$ $E = 0^b$	$^2A''$	125.5°	2336 (26), 728 (41), 537 (4), 214 (29)
$(N_2)Sc(O_2)$ $E = +27^b$	D		1879 (236), 868 (148), 619 (58), 585 (24)
$NNSc(O_2)$ $E = +30$	D		1950 (2040), 863 (89), 610 (22), 577 (30)
$NNScO_2$ $E = +63$	$^4A''$	1.937 Å 131.1°	2001 (415), 527 (124), 494 (4), 359 (1)
$NNSc(O_2)$ $E = +69$	$^4A'$		1881 (1540), 1126 (28), 482 (73), 406 (1)
$(N_2)ScOO$ $E = +70$	$^2A''$		1828 (508), 1160 (307), 570 (25), 378 (22)
$(N_2)Sc(O_2)$ $E = +94$	$^4B_1$		1688 (419), 1124 (30), 566 (75), 427 (7)

[a] Frequencies, cm^{-1} (infrared intensities, km/mol). [b] Relative energies in kcal/mol.

In the 900 cm^{-1} region the bands 922.0 cm^{-1} (weak), and 909.0 cm^{-1}(strong) were observed after deposition together with the weak 1109.5 cm^{-1} band from the upper region. Annealing increased the strong 909.0 cm^{-1} band and produced new satellites at 924.3, 921.8, 919.2, 916.3, 913.9, 912.0 cm^{-1} and a new band at 1106.9 cm^{-1}. The 900 cm^{-1} bands always produced doublets with the 16/18 ratio 1.0435, while the high-frequency bands 1109.5 and 1106.8 cm^{-1} produced doublets and triplets, respectively, with mechanical and statistical mixtures, and isotopic ratios 1.0599 and 1.0586. The positions of maxima of all bands in the 925−900 cm^{-1} region were shifted down and up, respectively, by 0.4 cm^{-1} in mixture experiments. This small shift is due to secondary isotopic splittings. A previous study assigned the 909.0 cm^{-1} band to a bent OScO molecule and suggested accidental degeneracy of ν_1 and ν_3 vibrations.[20] We disagree with this assignment and connect the 909.0 cm^{-1} band and satellites with the terminal Sc−O vibration of the $(O_2)ScO$ molecule. The observed secondary isotopic splittings are due to interaction between terminal and O−O vibrations in isotopically mixed molecules. The 1109.5/1106.9 cm^{-1} bands are due to the O−O vibration of this molecule. The satellites on both bands are due to different matrix sites. Experiments with N_2O produced the strong band at 894.9 cm^{-1} and satellites at 909.0, 906.7, 902.4 and 899.9 cm^{-1} and no bands in the high-frequency region. Nitrogen matrix experiments observed the strong 902.7/898.7 cm^{-1} doublet and satellites but no bands in the 1100 cm^{-1} region. The isotopic ratio for the latter doublet is 1.0436, near the diatomic value. Note that a weak 466.3 cm^{-1} band grew on annealing and produced doublet and triplet isotopic structures with evidence of secondary isotopic splittings to indicate weak coupling to a third inequivalent oxygen and the 16/18 ratio 1.0332. This band can be assigned to the "ν_2" vibration of the cyclic fragment in $(O_2)ScO$.

The analogous bands in the N_2O/Ar and O_2/N_2 systems at 894.9 and 898.7 cm^{-1} are due to $(N_2)ScO$ and $(N_2)_xScO$. Since the ScO molecule is essentially triple-bonded due to a dative interaction,[27] additional electron density from ligands such as O_2 or N_2 on Sc will decrease the dative bonding and result in a lowering of the Sc−O stretching frequency, as observed and calculated here. The behavior of $(N_2)_xScO$ at 898.7 cm^{-1} is identical with that of $(N_2)_xScN$ at 865.0 cm^{-1} in experiments with Sc in pure nitrogen.[39] Both bands were weak on codeposition, increased markedly on annealing, and decreased on photolysis (presumably expelling N_2 ligands). Apparently, the infrared intensity is increased upon the addition of N_2 ligands to ScO.

ScO_3. The strong bands that appeared on annealing at 818.6 and 804.0 cm^{-1} in solid argon and 811.7 in solid nitrogen produced quartet and sextet ozone-like isotopic structures with 16/18 ratios near 1.059. Similar bands were observed in the previous Sc work.[20] Assignment to the ν_3 mode of O_3^- in the $Sc^+O_3^-$ species follows. Such bands are characteristic of alkali and alkaline earth metal ozonides.[29,40,41] Note that these bands demonstrate the role of the +1 oxidation state for Sc, as was also found for Ca, and that there is little difference between the argon and nitrogen matrix environments for these species. The ScO_3 species is made from the reaction of ScO and O_2 on diffusion. Presumably addition to the oxygen end gives ScO_3 and reaction at scandium gives $(O_2)ScO$. In solid nitrogen the ozonide species may in fact be $(N_2)ScO_3$.

OScO. The 722.5 cm^{-1} band in argon experiments with O_2 and N_2O and the 710.2/705.4 cm^{-1} doublet with O_2 in nitrogen were produced on deposition and decreased on annealing. These bands gave doublet and triplet isotopic structures with mechanical and statistical mixed isotopic oxygen, which characterizes the vibration of two equivalent oxygen atoms, and the 16/18 ratios 1.0367 and 1.0374, which indicate an antisymmetric vibration. These bands are assigned to the ν_3 vibration of the symmetrical bent OScO molecule. Asymmetry in the statistical oxygen isotopic structure indicates that the symmetric vibration should be higher, but unfortunately no bands with a suitable isotopic ratio were detected in the 790−730 cm^{-1} region.

The 16/18 isotopic ratio for ν_3 enables a 133 ± 2° upper limit for the OScO valence angle in solid argon to be determined.[1,6,29,42] The ±0.1 cm^{-1} frequency accuracy defines the ±2° uncertainty. The nitrogen matrix upper limit, 128 and 130° for two sites, is essentially the same. In the OCrO case, an identical 132 ± 2° upper limit was determined from the 16/18 ratio with ^{52}Cr; however, resolution of chromium isotopic splitting enabled a 126° lower limit to be determined from the 52/53 ratio.[6] In the absence of scandium isotopic splittings, this comparison with OCrO suggests an angle of 128 ± 4° for OScO, assuming comparable anharmonicities in the ν_3 vibrations of OCrO and OScO, as the upper limit-lower limit separation is due to differences in anharmonicities between the vibrations of each isotopic molecule.[42] Although the valence angle is not changed significantly for OScO on going from a solid argon to a solid nitrogen environment, the frequency shift from 722.5 to 705.4 cm^{-1} (major site) suggests some ligation by N_2 at scandium.

DFT calculations provide some support for the identification of OScO. Stretching frequencies were predicted at 742 and 545 cm^{-1} for ν_1 and ν_3, respectively, and the valence angle at 126°. Although the calculated valence angle is in excellent agreement, the calculated ν_3 value is lower than observed.

Further attention must be paid to reaction mechanisms. Several gas-phase studies have found that ground-state Sc atoms react with dioxygen to form ScO molecules;[11,12,18] any OScO formed was not detected. The importance of collisonal stabilization of transition metal dioxide molecules during matrix condensation has been noted.[1−10] The matrix isolation experiments of Serebrennikov failed to produce and trap OScO (the 909 cm^{-1} band is reassigned here to $(O_2)ScO$) presumably owing to insufficient activation energy in the thermal Sc atoms employed.[20] The more energetic laser-ablated Sc atoms produced here have sufficient activation energy to insert into dioxygen, and we presume that metastable Sc atoms are particularly efficient in the insertion reaction. Reaction 3 is

$$Sc^* + O_2 \rightarrow [OScO]^* \xrightarrow{\text{argon}} OScO \qquad (3)$$

highly exothermic and dissipation of this energy by collision with argon atoms during the matrix condensation process is necessary for the stabilization of the OScO molecule. Note that OScO is also made in excess nitrogen and that the $NNScO_2$ complex makes little difference in the OScO frequencies (Table 3).

The OScO molecule has been observed in the gas phase by mass spectroscopy from reaction 4.[27] This work found that D_o(OSc−O) ≈ $0.6D_o$ (Sc−O), which is in accord with the frequencies assigned here.

$$ScO^+ + NO_2 \rightarrow OScO + NO^+ \qquad (4)$$

The relationship between symmetrical bent OCaO ($\nu_3 = 516$ cm^{-1}, $\alpha = 140 \pm 10°$), OScO ($\nu_3 = 722$ cm^{-1}, $\alpha = 128 \pm 4°$), and OTiO ($\nu_3 = 917$ cm^{-1}, $\alpha = 113 \pm 2°$) on one hand and CaO (747 cm^{-1}),[29] ScO (976 cm^{-1}), and TiO (988 cm^{-1})[1] on the other is of chemical interest. The increase in stability of higher oxidation states on going from OCaO to OScO to OTiO is clearly demonstrated. This is a result of the number of valence electrons; Ca can only form two single bonds in OCaO, while Ti, with four valence electrons, can form two double bonds in OTiO. Since Sc has three valence electrons, OScO is intermediate.

No bands in argon matrices can be associated with the ScOO and $Sc(O_2)$ molecules based on isotopic shifts. The previous assignment[20] of a 694 cm^{-1} band to $Sc(O_2)$ is not supported here; bands in this region will be assigned below to $(ScO)_2$. In contrast, open MOO molecules have been reported for the later transition metals Cr−Cu[2,3,6−10] and cyclic $M(O_2)$ molecules for Mn−Ni.[2,3,7−9] However, nitrogen matrix experiments produced several bands which are candidates for end- and side-bonded scandium dioxygen complexes where the role of nitrogen is important.

(N_2)ScOO. Bands at 1024.1 and 1011.0 cm^{-1} were observed on annealing and destroyed on photolysis; weak bands at 1828.2 and 1824.6 cm^{-1} shared this unique behavior. Doublet and quartet isotopic structures for the former bands suggest two inequivalent oxygen atoms, and the 16/18 ratio 1.0572 is suitable for an O−O vibration interacting with other mode. The latter bands are appropriate for side-bound N_2. These bands are assigned to the (N_2)ScOO molecule. DFT calculations predict these modes at 1828 and 1160 cm^{-1}. Although the O−O stretching mode is calculated some 140 cm^{-1} too high, the calculated oxygen isotopic quartet—1160, 1137, 1118, 1094 cm^{-1}—is in very good agreement with the observed band separations. Similar MOO molecules have been observed for the late first row transition metals, which had much smaller M−16−18, M−18−16 separations indicating less stretch, stretch interaction.[2,3,8−10]

It should be mentioned here that disappearance of (N_2)ScOO on photolysis is accompanied by growth of red wings on $(N_2)Sc(O_2)$ and $(NN)_xSc(O_2)$ absorptions. Previous work showed that less stable FeOO undergoes photochemical isomerization to $Fe(O_2)$.[2]

$(NN)_xSc(O_2)$ and $(N_2)Sc(O_2)$. The bands 1120.4/1119.4, 841.9, 614.6 and 602.8 cm^{-1} behaved similarly on photolysis and annealing. Each of them produced triplets with mechanical and statistical mixtures and intensity distributions 3:x:3 and 1:2:1, respectively, with x ranging from 0 to 2 on annealing after photolysis. In experiments with the mechanical isotopic mixture, intermediate components appeared after photolysis, which suggests a different mechanism for isotopic mixing than initial product formation. The 16/18 isotopic ratios 1.0597, 1.0549, 1.0352 and 1.0504 are suitable for the assignment of these bands to the ν_1, ν_1, ν_2, and ν_3 vibrations of a cyclic $Sc(O_2)$ molecule.

DFT calculations predict ν_1, ν_2, and ν_3 for doublet $Sc(O_2)$ at 882, 634 and 570 cm^{-1}. Similar calculations predicted 824, 620 and 500 cm^{-1} bands for $Ca(O_2)$, which may be compared to the 742, 556, 501 cm^{-1} observed values.[30] A similar correlation is evident with the above 841.9, 614.6 and 602.8 cm^{-1} bands, which are assigned here to $Sc(O_2)$ in solid nitrogen. Since coordination by N_2 has a small effect on the calculated frequencies, this species is better described as $(N_2)Sc(O_2)$, even though the N_2 mode was not detected.

Split bands at 2126.8/2125.3 cm^{-1} show the same appearance and behavior on annealing as the 1120.4/1119.4 cm^{-1} bands; the upper band shifted to 2056.2 cm^{-1} with $^{15}N_2$ as appropriate for a N−N stretching mode. Note that both frequencies are higher than calculated for doublet $NNSc(O_2)$ but the O−O mode is near that predicted for quartet $Sc(O_2)$ states. The best present description for this species is $(NN)_xSc(O_2)$ where extensive ligation by NN allows less charge transfer to O_2 more like that found in the quartet $Sc(O_2)$ molecule.

The photochemistry displayed in Figure 4 reveals a different mechanism than the initial route of formation during annealing. The observation of OScO and no $(N_2)Sc(O_2)$ on condensation in excess N_2 suggests that the more stable open dioxide is formed directly by insertion of energetic (metastable) Sc atoms; however, on annealing cold Sc instead adds to form the cyclic complex $(N_2)Sc(O_2)$ and the open complex (N_2)ScOO. Photolysis destroys the latter *and* $(NN)_x$ScO *and* ScO_3 and produces more $(N_2)Sc(O_2)$ and $(NN)_xSc(O_2)$ including the $^{16}O^{18}O$ isotopic species *not present* on deposition in the $^{16}O_2 + {}^{18}O_2$ experiment. This means that the ozonide photolyses to give product and O atoms which diffuse and react to form more product, reactions 5 and 6.

$$N_2 + ScO_3 \rightarrow (N_2)ScO_3 \xrightarrow{\text{photolysis}} (N_2)Sc(O_2) + O \qquad (5)$$

$$(NN)_xScO + O \rightarrow (NN)_xSc(O_2) \qquad (6)$$

The photodissociation of ozone also contributes O atoms for reaction 6. The spectrum in Figure 4c shows the increase of ozone 16−18−16 and 18−16−18 bands at 1010 and 1020 cm^{-1}, respectively, at the expense of stronger ozone 16−16−16, 16−16−18, 16−18−18, 18−18−18 bands.[43] This clearly demonstrates the diffusion and reaction of O atoms during photolysis. This photochemical isotopic equilibration also occurs for ScO_3.

ScOSc. The 892.9 cm^{-1} band in argon was observed after deposition and decreased on annealing; it increased relative to ScO in experiments with higher laser energy. This absorption produced sharp doublet isotopic structure with both mechanical and statistical mixtures with no evidence of secondary isotopic shifts. The 16/18 ratio 1.0500 is very close to that expected for the ν_3 vibration of a linear ScOSc molecule (1.0509). Thus, the 892.9 cm^{-1} band is assigned to scandium suboxide with a linear (or near linear) structure like aluminum suboxide,[44] which has a ν_3 fundamental at 993 cm^{-1}. Note that appearance of linear suboxides in the metal−oxygen systems is characteristic of group III elements. In experiments with N_2O as well as in nitrogen films, Sc_2O was not detected probably due to overlapping with strong bands of $(N_2)_x$ScO complexes.

ScOScO. The weak 866.0 cm^{-1} band in argon shifted to 828.7 cm^{-1} giving a 16/18 ratio slightly higher than the diatomic value. Mechanical isotopic mixtures gave the same bands, but the statistical mixture gave broadened bands at 865.5 and 830.3 cm^{-1} with clear evidence of a secondary isotopic effect and two inequivalent oxygen atoms. This evidence suggests the open ScOScO dimer; the analogous molecule was observed for aluminum.[44]

$(ScO)_2$. Bands at 699.1 and 647.8 cm^{-1} in argon were weak in the deposited samples and increased on annealing. These bands shifted to 670.1 and 622.5 cm^{-1} with $^{18}O_2$ giving near diatomic ratios, and triplets were produced with the statistical isotopic mixture indicating two equivalent oxygen atoms. These bands are assigned to the ring dimer $(ScO)_2$ molecule. The small differences from the diatomic 16/18 ratio may suggest a nonplanar structure, which was also observed for $(TiO)_2$.[1] The observed doublet structure with mechanical isotopic mixtures suggests secondary reaction 7 for the formation of this dimer.

$$OScO + Sc \rightarrow (ScO)_2 \qquad (7)$$

Dimerization of ScO is a less-probable mechanism here owing to the reactivity of ScO with O_2 to form (O_2)ScO and ScO_3. Analogous bands in the nitrogen experiments at 688.1 and 635.5 cm^{-1} are assigned to $(ScO)_2$ as well; the effect of ligation by N_2 is minimal.

$Sc(O_2)_2$. The strong bands in the 550 cm^{-1} region in argon appeared in the spectra after annealing. Experiments with the mechanical isotopic mixture found a triplet, and the scrambled oxygen isotopic structure was not completely resolved due to band overlapping. The 16/18 ratio 1.0304 is unusually low. The same low ratio was obtained for the $Ca(O_2)_2$ molecule with D_{2d} symmetry.[30] According to DFT calculations, this molecule should have only one strong fundamental with a low oxygen ratio. Thus, based on comparison with the Ca + O_2 system, bands in the 550 cm^{-1} region are assigned to the analogous $Sc(O_2)_2$ molecule with D_{2d} symmetry.[30]

Other Absorptions. Charged species are observed in these experiments, but such high oscillator strength species play a minor overall role. The weak 1118 and 953.8 cm^{-1} bands are due to O_4^+ and O_4^- in solid argon and the 990.7 cm^{-1} band is due to O_4^- in solid nitrogen.[45−47]

In nitrogen matrix reactions, some NO and NO_2 is formed,[38] and reaction with scandium gives the Sc^+NO^- and $Sc^+NO_2^-$ species, which are identified from isotopic shifts.[48,49]

Weak bands appear at 1554.3 cm^{-1} on annealing in solid argon, near the pure oxygen value.[14] These bands show triplet scrambled isotopic splitting and the 16/18 ratio 1.0594 for a pure O−O stretching mode. These bands are due to a weak (O_2) complex with some molecule appearing on annealing; the high-spin $Sc^+O_3^-$ scandium ozonide species is a possibility.

Conclusions

Reaction of laser-ablated Sc atoms and oxygen molecules produced ScO and OScO as primary products, which were identified by oxygen isotopic shifts and splittings. The ScO molecule has two sites in argon matrixes—blue- and red-shifted 10−11 cm^{1} from the gas-phase frequency. The bent OScO molecule (128 ± 4°) is formed by reaction of metastable Sc atoms and oxygen; ground state Sc apparently does not insert into the oxygen molecule. In solid nitrogen end and side-bonded isomers of ScO_2 can be formed as dinitrogen complexes; (N_2)-ScOO is very photosensitive and photolytically isomerizes to $(N_2)Sc(O_2)$. The later molecule is a peroxide type complex as its fundamental O−O vibration is about 842 cm^{-1} and analogous to $Ca(O_2)$.[29,30] Secondary reactions lead to the formation of ScO_3, $(ScO)_2$, $Sc(O_2)_2$ and complexes of ScO with O_2. These products were also identified by isotopic shifts and splittings.

In contrast to OTiO whose stretching frequencies are just lower than the TiO fundamental,[1] the ν_3 fundamental for OScO (722 cm^{-1}) is substantially lower than the ScO fundamental (976 cm^{-1}). Clearly, Sc can support one but not two strong bonds to oxygen as found in gas phase thermochemical studies.[27] Scandium is more like calcium as shown by the frequencies for CaO (747 cm^{-1}) and OCaO (516 cm^{-1}).[29]

Acknowledgment. We thank W. D. Bare for assistance with the experiments.

References and Notes

(1) Chertihin, G. V.; Andrews, L. *J. Phys. Chem.* **1995**, *99*, 6356.

(2) Chertihin, G. V.; Saffel, W.; Yustein, J. T.; Andrews, L.; Neurock, M.; Ricca, A.; Bauschlicher, C. W., Jr. *J. Phys. Chem.* **1996**, *100*, 5261.

(3) Andrews, L.; Chertihin, G. V.; Ricca, A.; Bauschlicher, C. W., Jr. *J. Am. Chem. Soc.* **1996**, *118*, 467.

(4) Chertihin, G. V.; Andrews, L. *J. Chem. Phys.* **1997**, *106*, 3457.

(5) Chertihin, G. V.; Bare, W. D.; Andrews, L. *J. Phys. Chem. A* **1997**, *101*, 5090.

(6) Chertihin, G. V.; Bare, W. D.; Andrews, L. *J. Chem Phys.* **1997**, *107*, 2798.

(7) Chertihin, G. V.; Andrews, L. *J. Phys. Chem. A* **1997**, *101*, 8547.

(8) Chertihin, G. V.; Citra, A.; Andrews, L.; Bauschlicher, C. W., Jr. *J. Phys. Chem. A* **1997**, *101*, 8793.

(9) Citra, A.; Chertihin, G. V.; Andrews, L.; Neurock, M. *J. Phys. Chem. A* **1997**, *101*, 3109.

(10) Chertihin, G. V.; Andrews, L.; Bauschlicher, C. W., Jr. *J. Phys. Chem. A* **1997**, *101*, 4026.

(11) Stringat, R.; Athenour, C.; Femenias, J.-L. *Can. J. Phys.* **1972**, *50*, 395.

(12) Chalek, C. L.; Gole, T. L. *J. Chem. Phys.* **1976**, *65*, 2845.

(13) Gole, T. L.; Preuss, D. R. *J. Chem. Phys.* **1977**, *66*, 3000.

(14) Huber, K. P.; Herzberg, G. *Constants of Diatomic Molecules*; Van Nostrand Reinhold: New York, 1979.

(15) Merer, A. J. *Annu. Rev. Phys. Chem.* **1989**, *40*, 407.

(16) Childs, W. J.; Steimle, T. *J. Chem. Phys.* **1988**, *88*, 6188.

(17) Shirley, J.; Scurlock, C.; Steimle, T. *J. Chem. Phys.* **1990**, *93*, 1568.

(18) Ritter, D.; Weisshaar, T. C. *J. Phys. Chem.* **1990**, *94*, 4907.

(19) Weltner, W., Jr.; McLeod, D., Jr.; Kasai, P. H. *J. Chem. Phys.* **1967**, *46*, 3172.

(20) Konnov, S. A.; Serebrennikov, L. V.; Maltsev, A. A. *Vestn. Mosk. University Ser. 2, Khim* **1982**, *101*. Serebrennikov, L. V., Dr. Science Thesis, Moscow State University, 1990.

(21) Kauffman, T. W.; Hauge, R. H.; Hargrave, T. L. *J. Phys. Chem.*, **1985**, *89*, 3541.

(22) Bauschlicher, C. W., Jr.; Langhoff, S. R. *J. Chem. Phys.* **1986**, *85*, 5936.

(23) Dolg, M.; Wedig, U.; Stoll, H.; Preuss, H. *J. Chem. Phys.* **1987**, *86*, 2123.

(24) Hattan, S. M. *J. Phys. Chem.* **1993**, *97*, 3171.

(25) Bauschlicher, C. W., Jr.; Maitre, P. *Theor. Chim. Acta* **1995**, *90*, 189.

(26) Kordis, J.; Gingerich, K. A. *J. Chem. Phys.* **1977**, *66*, 483.

(27) Clemmer, D. E.; Dalleska, N. F.; Armentrout, P. B. *Chem. Phys. Lett.* **1992**, *190*, 259.

(28) Thiem, T. L.; Salter, R. H.; Gardner, J. A. *Chem. Phys. Lett.* **1994**, *218*, 309.

(29) Andrews, L.; Yustein, J. T.; Thompson, C. A.; Hunt, R. D. *J. Phys. Chem.* **1994**, *98*, 6514.

(30) Andrews, L.; Chertihin, G. V.; Thompson, C. A.; Dillon, J; Byrne, S.; Bauschlicher, C. W., Jr. *J. Phys. Chem.* **1996**, *100*, 10088.

(31) *Gaussian 94, Revision B.1*. Frisch, M. J.; Trucks, G. W.; Schlegel, H. B.; Gill, P. M. W.; Johnson, B. G.; Robb, M. A.; Cheeseman, J. R.; Keith, T.; Petersson, G. A.; Montgomery, J. A.; Raghavachari, K.; Al-Laham, M. A.; Zakrzewski, V. G.; Ortiz, J. V.; Foresman, J. B.; Cioslowski, J.; Stefanov, B. B.; Nanayakkara, A.; Challacombe, M.; Peng, C. Y.; Ayala, P. Y.; Chen, W.; Wong, M. W.; Andres, J. L.; Replogle, E. S.; Gomperts, R.; Martin, R. L.; Fox, D. J.; Binkley, J. S.; Defrees, D. J.; Baker, J.; Stewart, J. P.; Head-Gordon, M.; Gonzalez, C.; Pople J. A. Gaussian, Inc., Pittsburgh, PA, 1995.

(32) Frisch, M. J.; Pople, J. A.; Binkley, J. S. *J. Chem. Phys.* **1984**, *80*, 3265 and references therein.

(33) Wachters, A. J. H. *J. Chem. Phys.* **1970**, *52*, 1033.

(34) Hay, P. J. *J. Chem. Phys.* **1977**, *66*, 4377.

(35) Becke, A. D. *Phys. Rev. A* **1988**, *38*, 3098, Perdew, J. P. *Phys. Rev. B* **1986**, *33*; **1986**, *34*, 7406(E). and Vosko, S. H.; Wilk, L.; Nusair, M. *Can. J. Phys.* **1980**, *58*, 1200, for the nonlocal exchange, nonlocal correlation, and local correlation, respectively.

(36) Becke, A. D. *J. Chem. Phys.* **1993**, *98*, 5648.

(37) Stephens, P. J.; Devlin, F. J.; Chablowski, C. F.; Frisch, M. J. *J. Phys. Chem.* **1994**, *98*, 11623.

(38) Andrews, L.; Chertihin, G. V.; Citra, A.; Neurock, M. *J. Phys. Chem.* **1996**, *100*, 11235.

(39) Chertihin, G. V.; Andrews, L.; Bauschlicher, C. W., Jr., to be published.

(40) Ault, B. S.; Andrews, L. *J. Chem. Phys.* **1975**, *62*, 2312, 2320.

(41) Spiker, R. C., Jr.; Andrews, L. *J. Chem. Phys.* **1973**, *59*, 1851.

(42) Allavena, M.; Rysnik, R.; White, D.; Calder, V.; Mann, D. E. *J. Chem. Phys.* **1969**, *50*, 3399.

(43) Andrews, L.; Spiker, R. C., Jr. *J. Phys. Chem.* **1972**, *76*, 3208.

(44) Andrews, L.; Burkholder, T. R.; Yustein, J. R. *J. Phys. Chem.* **1992**, *96*, 10182

(45) (a) Andrews, L. *J. Chem. Phys.* **1971**, *54*, 4935. (b) Thompson, W. E.; Jacox, M. E. *J. Chem. Phys.* **1989**, *91*, 3826. (c) Hacaloglu, J; Andrews, L., to be published.

(46) The weak 1118 cm^{-1} band is due to O_4^+; see ref 45b.

(47) Chertihin, G. V.; Andrews, L. *J. Chem. Phys.* **1996**, *105*, 2561.

(48) Milligan, D. E.; Jacox, M. E. *J. Chem. Phys.* **1971**, *55*, 3404.

(49) Tevault, D. E.; Andrews, L. *Chem. Phys. Lett.* **1977**, *48*, 103.